Accepted Manuscript

Synthesis and biological evaluation of 6-fluoro-3-phenyl-7-piperazinyl quinolone derivatives as potential topoisomerase I inhibitors

Raoling Ge, Qian Zhao, Zhouling Xie, Lu Lu, Qinglong Guo, Zhiyu Li, Li Zhao

PII: S0223-5234(16)30544-X

DOI: 10.1016/j.ejmech.2016.06.054

Reference: EJMECH 8715

To appear in: *European Journal of Medicinal Chemistry*

Received Date: 2 March 2016

Revised Date: 27 June 2016

Accepted Date: 28 June 2016

Please cite this article as: R. Ge, Q. Zhao, Z. Xie, L. Lu, Q. Guo, Z. Li, L. Zhao, Synthesis and biological evaluation of 6-fluoro-3-phenyl-7-piperazinyl quinolone derivatives as potential topoisomerase I inhibitors, *European Journal of Medicinal Chemistry* (2016), doi: 10.1016/j.ejmech.2016.06.054.

This is a PDF file of an unedited manuscript that has been accepted for publication. As a service to our customers we are providing this early version of the manuscript. The manuscript will undergo copyediting, typesetting, and review of the resulting proof before it is published in its final form. Please note that during the production process errors may be discovered which could affect the content, and all legal disclaimers that apply to the journal pertain.

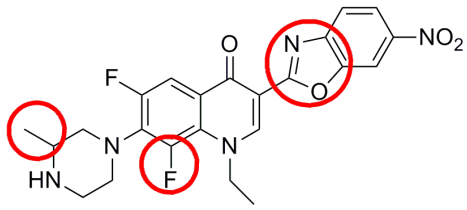

5

simplify

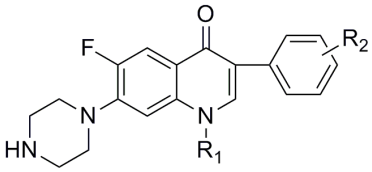

R_1 = ethyl, cyclopropyl
R_2 = H, F, Cl, CN, OCH3

Top I Activity

screen

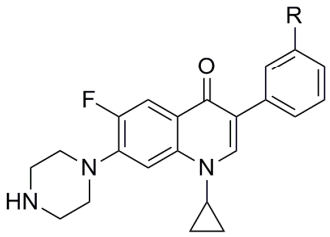

Effect on DNA Distribution in A549 Cells

Inhibits the growth of A549 tumor xenografts in nude mice

18f:R=Cl IC50 = 0.89 μ M (Hela)
0.61 μ M (BGC-823)
0.86 μ M (HepG2)
0.11 μ M (A549)

18g:R=OCH_3 IC50 = 0.92 μ M (Hela)
0.69 μ M (BGC-823)
0.91 μ M (HepG2)
0.12 μ M (A549)

ACCEPTED

ACCEPTED MANUSCRIPT

Synthesis and Biological Evaluation of 6-fluoro-3-phenyl-7-piperazinyl Quinolone Derivatives as Potential Topoisomerase I Inhibitors

Raoling Ge[a], Qian Zhao[a], Zhouling Xie[a], Lu Lu[b], Qinglong Guo[b], Zhiyu Li[a*] , Li Zhao[b*]

[a] *Jiangsu Key Laboratory of Drug Design and Optimization, China Pharmaceutical University, 24 Tongjiaxiang, Nanjing 210009, The People's Republic of China*

[b] *Jiangsu Key Laboratory of Carcinogenesis and Intervention, China Pharmaceutical University, 24 Tongjiaxiang, Nanjing 210009, The People's Republic of China*

[*]Corresponding author. Zhiyu Li, tel: +86 13951678592; e-mail: zhiyuli@cpu.edu.cn

[*]Corresponding author. Li Zhao, tel: +86 13851847586; e-mail: zhaoli@cpu.edu.cn

Abstract:

The design and synthesis of a new series of 6-fluoro-3-phenyl-7-piperazinyl quinolone derivatives, built on the structure of 1-ethyl-3-(6-nitrobenzoxazol-2-yl)-6,8-difluoro-7-(3-methylpiperazin-1-yl)-4(1H)-quinolone, are described. These compounds provide new scaffold for the discovery of Topoisomerase I (Top I) inhibitors and target based assay showed that they can obviously inhibited Top I at 100 μM. The *in vitro* anti-proliferative activity of these new compounds was evaluated against A549, Hela, BGC-823, and HepG2 cell lines. Compounds **18a**-**g** showed potent inhibitory activity against the growth of those cancer cell lines. The most positive compounds **18f** and **18g** demonstrated as potent as camptothecin in Top I inhibition assay and MTT assay. Compounds **18f** and **18g** led to an obvious increase in the percentage of S phase of the cells in 24 h. The *in vivo* data showed that **18f** and **18g** inhibited tumor growth with the inhibitory rate of 29.25% and 42.75% at 20 mg/kg, respectively. The data suggested the therapeutic potential for further development.

Keywords: quinolone derivatives, synthesis, Top I inhibitors, anti-proliferative activity

Corresponding author. Zhiyu Li, tel: +86 13951678592; e-mail: zhiyuli@cpu.edu.cn

Corresponding author. Li Zhao, tel: +86 13851847586; e-mail: zhaoli@cpu.edu.cn

1. Introduction

DNA topoisomerase I (Top I) is a ubiquitous DNA-cleaving enzyme which cuts one strand of a DNA double helix to relax supercoiled DNA for transcription, replication, and mitosis [1]. Top I works by uncoiling natural supercoiled DNA, transiently breaking one of the two strands of DNA, make another single chain pass through the gap, followed by religation of the broken strand, thus Top I changes supercoiling of DNA or helix insufficient [2]. Top I plays a critical role in the proliferation of cancer cells, and it is recognized as an important target to prevent rapid proliferation of cancer cells. Therefore, the discovery of new Top I inhibitors has attracted the attention of medicinal chemist throughout the world.

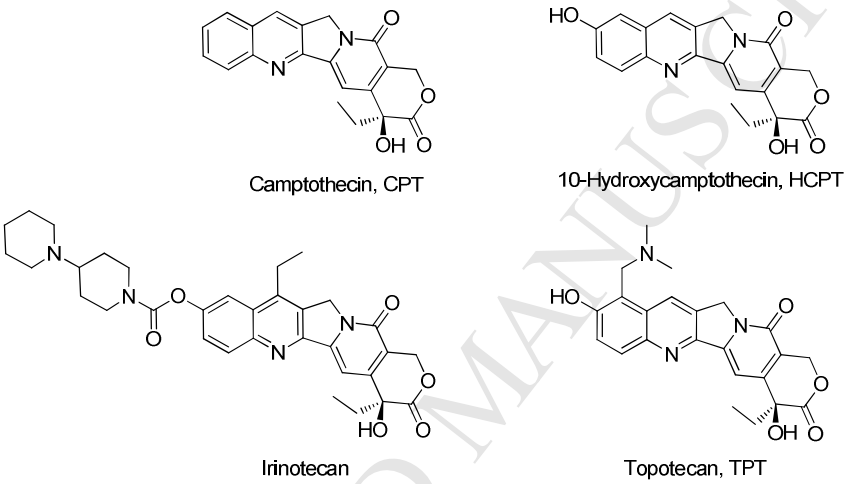

Figure 1. Structure of Camptothecin, 10-Hydroxycamptothecin, Irinotecan and Toptecan.

Camptothecin (CPT, **1**, **Figure 1**), a specific inhibitor of Top I, is widely used in clinics for its curative effect on a wide range of cancer cell lines. Unfortunately, the clinic utility of **CPT** is hampered by several disadvantages such as poor aqueous solubility and high toxicity [3]. As a result, these problems promoted further development of more water-soluble analogues, such as 10-hydroxycamptothecin (HCPT, **2**), irinotecan (**3**) and topotecan (TPT, **4**, **Figure 1**). Irinotecan and topotecan, which are the only current FDA-approved Top I inhibitors as anticancer drugs, are in clinical treatment [4-7]. However, the usage of **CPT** and its analogues was hindered by its rapid inactivation, which was derived from the rapid hydrolysis of the lactone ring under physiological condition [8]. As Top I is proven to be an effective target for cancer treatment, a slice of metabolically stable non-CPT Top I inhibitors with better pharmacokinetic features have been developed [9-14], like indolocarbazoles [13] and indenoisoquinolines (**Figure 2**) [14], some of them are now in clinical assessment [8]. Therefore, in our present study, we made great efforts to improve their chemical stability and biological activity.

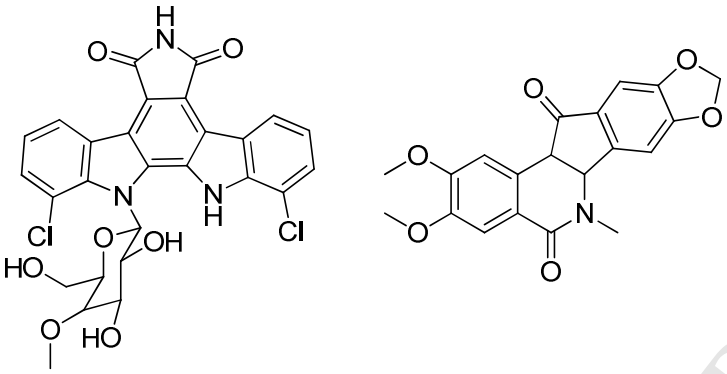

Figure 2. Structure of Rebeccamycin and NSC 314622.

2. Results and discussion

2.1 Design

With a view to the successful clinic utility of these non-CPT Top I inhibitors, we ascribe the better chemical stability with longer lifetimes of the trapped cleavage complex to the disappearance of a lactone ring in their skeleton [15]. It is well known that fluoro atom prolongs the half-life to improve the metabolic characteristics and piperazine or methyl piperazine increases the water solubility of compounds [3]. In 2009, our group discovered a novel series of Top I inhibitors with quinolone scaffold. 1-ethyl-3-(6-nitrobenzoxazol-2-yl)-6,8-difluoro-7-(3-methylpiperazin-1-yl)-4(1H)-quinolone (**5, Figure 3**) was the most potent compound we synthesized [3]. We also further improved biological activity and water solubility. Using a scaffold modification strategy, our team changed the 6-nitrobenzoxazol group into phenyl with different substituent groups. As F atom at the 8-position had little effect to enhance cytotoxicity and a methyl group on the piperazine substituent reduced cytotoxicity [3], we removed them to simplify the structure (**Figure 3**). Besides, the NH in quinolone was also substituted with ethyl and cyclopropyl. Herein we identified a suite of quinolone derivatives as potential Top I inhibitors.

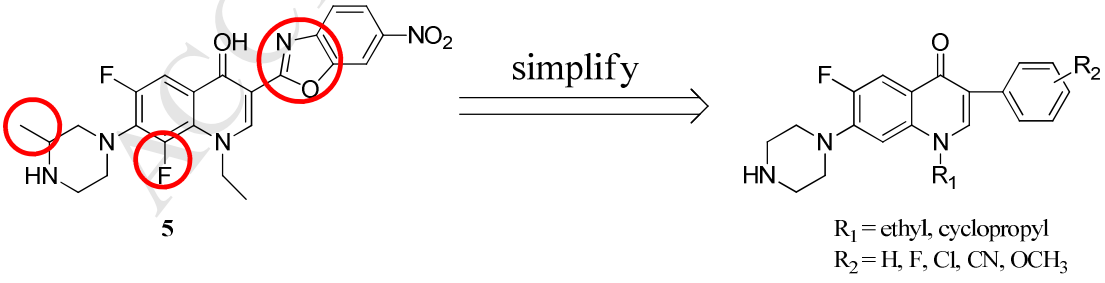

Figure 3. Compound generation by scaffold modification.

2.2 Chemistry

The synthesis of quinolone derivatives **17a-h**, **18a-i** is described in **Scheme 1**. Decarboxylation of **6**, **7** by reacting with concentrated hydrochloric acid led to intermediate **8**, **9**. In the presence of

bromine and acetic acid, 3-H was substituted by bromine to form **10**, **11**. Butyloxycarbonyl and methyl were introduced to piperazine to get intermediates **12**, **13** and **14**. Afterwards, **12**, **13** and **14** were subsequently coupled with different substituted phenylboronic acids to give rise to compounds **15a-h**, **16a-g** and **18h-i**. Then butyloxycarbonyl was removed by refluxing in the acetic acid to provide **17a-h, 18a-g**.

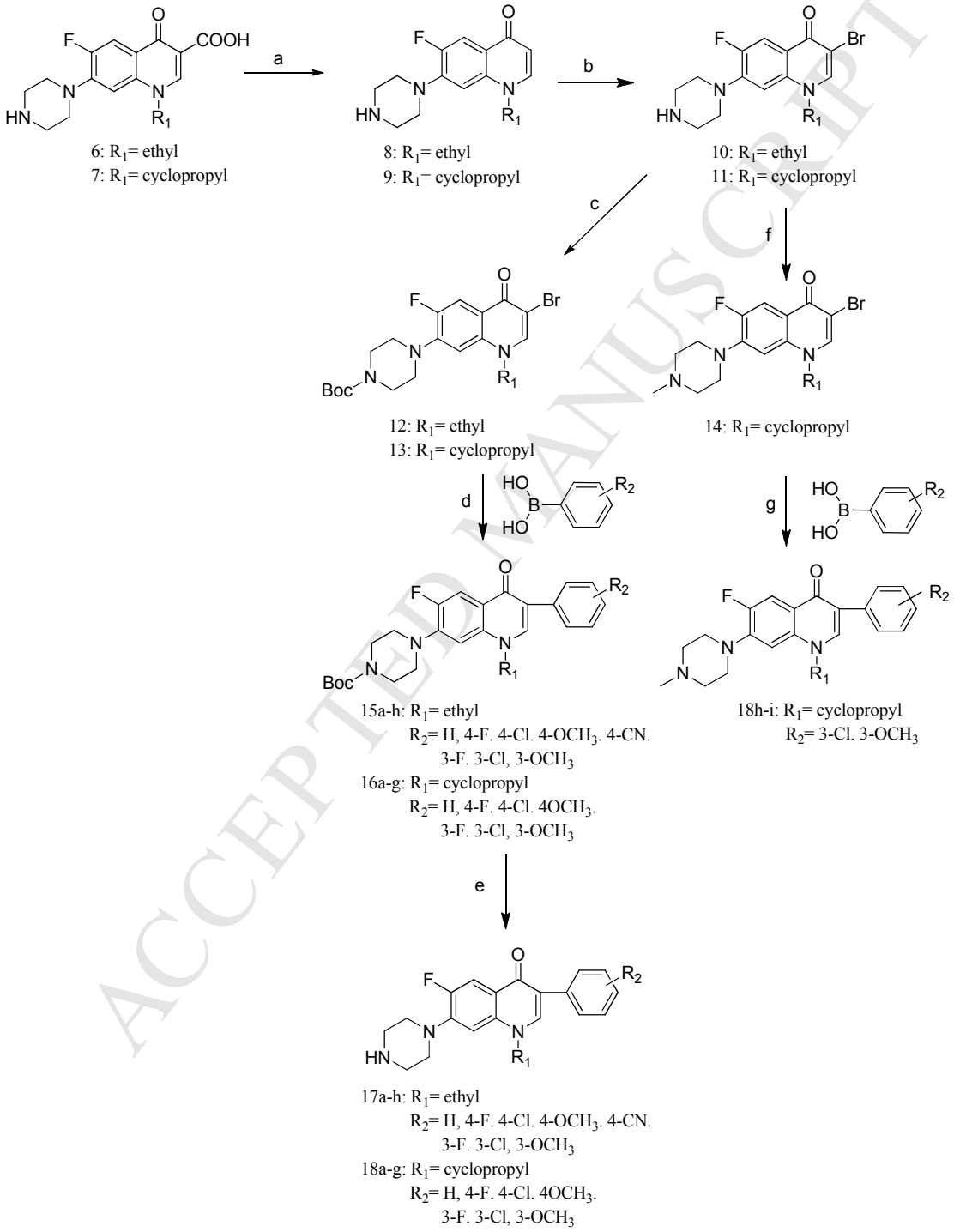

Scheme 1. Synthesis of quinolone derivatives. Reagents and conditions: (a) con.HCl, reflux, 24h, 98%; (b) CH_3COOH, Br_2, 25 □, overnight, 95%; (c) $(Boc)_2O$, Et_3N, CH_2Cl_2, 25 □, overnight, 95%; (d)

Toluene, MeOH, H_2O, K_2CO_3, $Pd(PPh_3)_4$, N_2, reflux, 2h, 80-90%; (e) CH_3COOH, reflux, 6h, 80-90%; (f) CH_3I, NaOMe, -10 □, overnight, 60%; (g) Toluene, MeOH, H_2O, K_2CO_3, $Pd(PPh_3)_4$, N_2, reflux, 2h, 80-90%.

2.3 Results and discussions

2.3.1 MTT assays

To explore the *in vitro* antiproliferative activity of all quinolone derivatives, 1-N-methyl-5-thiotetrazole (MTT) assay was used in four human cancer cell lines such as Hela (cervical adenocarcinoma), BCG-823 (gastric carcinoma), HepG2 (human hepatocellular liver carcinoma) and A549 (non-small cell lung carcinoma) with **CPT** as a positive control compound.

Table 1. The structures and the *in vitro* cytotoxic activities of quinolone derivatives.

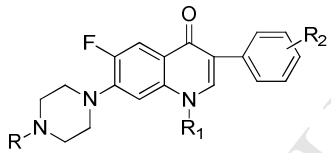

Compounds	***R***	***R₁***	***R₂***	**Antitumor cell proliferation (IC_{50}, μM)**			
				Hela	BGC-823	HepG2	A549
CPT				1.41±0.22	1.27±0.11	1.52±0.22	0.46±0.05
5				2.98±0.24	2.74±0.27	2.65±0.21	1.47±0.14
17a	H	ethyl	H	35.12±2.11	75.41±9.11	30.11±2.76	10.84±1.71
17b	H	ethyl	4-F	60.93±3.98	69.59±8.31	56.20±5.09	11.39±1.13
17c	H	ethyl	4-Cl	15.39±2.01	14.60±0.88	24.00±3.06	1.25±0.08
17d	H	ethyl	4-OCH_3	69.04±6.02	46.10±5.91	57.91±4.78	11.63±1.53
17e	H	ethyl	4-CN	14.64±2.01	18.66±1.33	12.60±1.02	1.09±0.07
17f	H	ethyl	3-F	21.95±1.62	27.27±3.11	27.80±2.21	3.06±0.43
17g	H	ethyl	3-Cl	16.07±1.97	18.37±2.02	15.26±1.49	0.78±0.05
17h	H	ethyl	3-OCH_3	12.19±0.99	14.73±1.21	13.02±1.55	0.80±0.11
18a	H	cyclopropyl	H	9.99±0.87	7.86±0.63	8.65±1.01	0.50±0.04
18b	H	cyclopropyl	4-F	14.86±1.54	15.11±1.94	10.57±0.99	1.68±0.08
18c	H	cyclopropyl	4-Cl	9.30±1.01	12.92±1.49	8.02±0.76	0.65±0.05
18d	H	cyclopropyl	4-OCH_3	16.47±1.95	18.90±2.09	20.76±1.99	1.87±0.26

18e	H	cyclopropyl	3-F	9.16±1.03	12.04±1.31	7.38±0.44	1.10±0.08
18f	H	cyclopropyl	3-Cl	0.89±0.04	0.61±0.08	0.86±0.10	0.11±0.01
18g	H	cyclopropyl	3-OCH_3	0.92±0.11	0.69±0.03	0.91±0.11	0.12±0.01
18h	methyl	cyclopropyl	3-Cl	15.83±1.09	20.17±1.39	26.49±2.05	1.34±0.11
18i	methyl	cyclopropyl	3-OCH_3	14.78±1.09	20.92±0.99	25.38±1.93	1.12±0.10

The results are reported as mean value ± SEM, n = 3.

Table 1 lists cytotoxic activities of two main skeleton quinoline derivatives. In different substituted groups to the phenyl ring, the data manifested that 4-substituted compounds follow this trends: -CN, -Cl > -H, -F, -OCH_3. However, this is not suitable for 3-substituted compounds. By comparing the different substituent positions, the substitution scaffolds at the 3-position and 4-position of phenyl have distinct effects on the biological activities of the molecules. Among these compounds, a quinolone nucleus with a 3-substituted phenyl, had an IC_{50} range of 0.11-27.80 μM, better than other compounds containing a 4-substituted ones, showing that the 3-substituted phenyl quinolone derivatives were more preferred, which may be due to steric-hindrance effect. We presumed that piperazine was crucial to cytotoxicity, then compounds **18h** and **18i** with 4-methyl piperazine at the 7-position were synthesized and evaluated. The IC_{50} values of compounds **18h** and **18i** were immensely decrease comparing with **18f** and **18g** as expected, supporting that piperazine substituted compounds yield preferable cytotoxicity than 4-methyl piperazine ones. Notably, cyclopropyl substituted compounds were more cytotoxic than ethyl substituted ones, which is in coincidence with the basic skeletons. Compounds **18f** and **18g**, whose biological activities were greatly improved, were discovered to be the best of all compounds we synthesized, with IC_{50} values of 0.89, 0.92 μM (Hela), 0.61, 0.69 μM (BCG-823), 0.86, 0.91 μM (HepG2) and 0.11, 0.12 μM (A549) respectively, which is as potent as **CPT** in the biological assay. Further data showed that almost all the compounds induced stronger growth inhibitory effect on A549 cells than on another cancer cells in MTT assay.

2.3.2 Top I activity

To explore the mechanism by which compounds inhibited Top I and thereby caused cytotoxicity, seven compounds with the best anti-proliferation activity (**18a-g**) were examined at 100 μM by measuring the relaxation of supercoiled DNA of plasmid pBR322 with **CPT** as positive control. The inhibitory activities on Top I of all the tested compounds were as potent as **CPT**, which coincided with the antiproliferative activities in MTT assay. In the Top I assay, IC50 values were much higher than in the cytotoxy assays. We speculated that an anti-proliferative activity of 18a-g might be only partially dependent on Top I, indicating that 18a-g had additional targets besides Top I. At higher concentrations of 50 μM, compound **5** was precipitated out under typical assay conditions. However, the solubility of

our compounds is higher than 400 μM, indicating that the solubility of our compounds was improved.

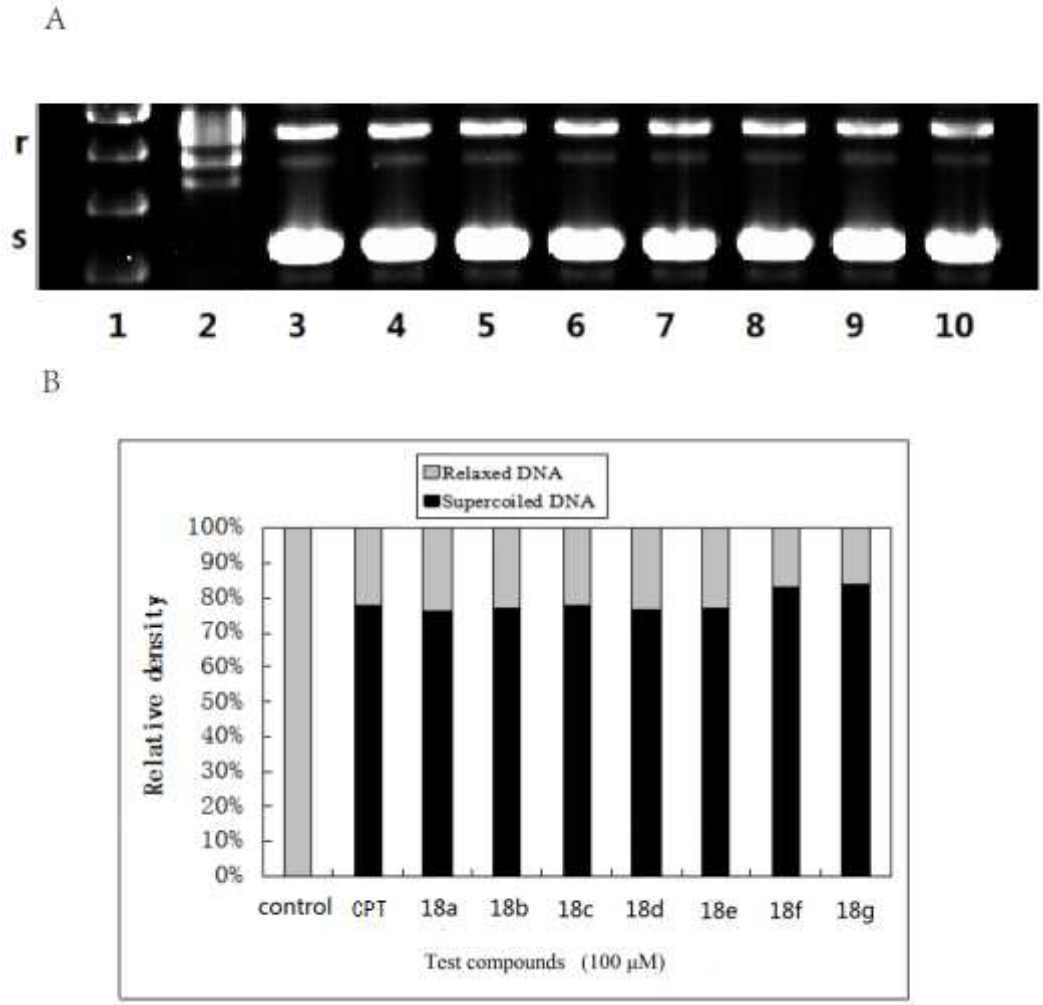

Figure 4. Effects of quinolone derivatives on Top I-mediated DNA relaxation activity. (A) Lane 1: marker; Lane 2: Top I + supercoiled pBR322 DNA (ScDNA); Lane 3: Top I + ScDNA + **CPT**; Lane 4: Top I + ScDNA + compound **18a**; Lane 5: Top I + ScDNA + compound **18b**, Lane 6: Top I + ScDNA + compound **18c**; Lane 7: Top I + ScDNA + compound **18d**; Lane 8: Top I + ScDNA + compound **18e**; Lane 9: Top I + ScDNA + compound **18f**; Lane 10: Top I + ScDNA + compound **18g**. (B) Effects of test compounds on Top I-mediated DNA relaxation. The proportion of relaxed DNA to the total DNA was measured by scanning with an imaging system. Bars show the percentage of supercoiled vs relaxed DNA. Marker: product of Tanon, China. R for relax pBR322 DNA and s for supercoiled pBR322 DNA.

2.3.3 Docking study

Based on molecular docking, we compared **18g** with **CPT** to reveal the binding mode of them with Top I/DNA binary complex (PDB ID: 1K4T). As shown in **Figure 5**, **18g** and **CPT** overlapped and had similar positions and orientations, lending support to the view that **18g** is Top I inhibitor as **CPT**. It could be found that the Pi interactions of **18g** and **CPT** within the complex were similar.

Nonetheless, they interacted with Top I/DNA binary complex in different patterns. Compound **18g** is capable of making two hydrogen bonding interactions to enhance the stabilization of the complex, illustrated as green dashed lines in **Figure 5**. The 4-position carbonyl oxygen of **18g** is shown to form a hydrogen-bonding with the guanidine protons of Arg364 and this have been previously reported for indenoisoquinoline analogues [16-18].The NH of the 7 position piperazine group of **18g** participated in hydrogen bonding with Glu356, further explained that piperazine is crucial for enhancing antineoplastic activity because it may increase the binding affinity of the inhibitors with Top I/DNA binary complex.

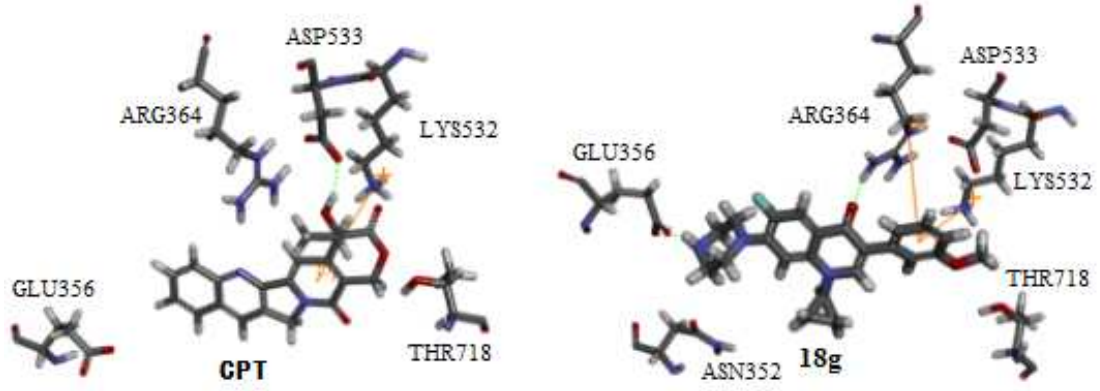

Figure 5. Docking results of **CPT** and **18g** with Top I/DNA binary complex. Energy-minimized hypothetical top-ranked binding pose of **CPT** and **18g** (colored by atom type). The stereoview is programmed for wall-eyed (relaxed) viewing. Top I amino acid residues not involved in bonding interactions have been removed to improve clarity. Hydrogen bonds are indicated by green dashed lines. Pi interactions are indicated by orange lines. Protein and compounds represented in stick model.

*2.3.4 Effect of **18f** and **18g** on DNA distribution in human non-small lung cancer A549 cells*

Previous works in rapidly proliferating cells revealed that the cytotoxicity of the famous Top I inhibitor, **CPT**, depended on active DNA replication [19]. Based on compound **18f** and **18g** showed positive activity in MTT assay and Top I inhibition assay, we further evaluated the effect of **18f** and **18g** on the distribution of the cells in cell cycle with **CPT** as positive control. Synchronized A549 cells treated with 0.5 μM **CPT**, **18f** and **18g** were performed to the flowcytometric analysis (**Figure 6**). **18f** and **18g** (0.5 μM) led to an obvious increase in percentage of cells in S phase at 24 h. The data showed that the percentage of cells in S phase was increased by around 20% at 0.5 μM at 24 h, as compared with the untreated group. However, the effects of the compounds were weaker than **CPT**.

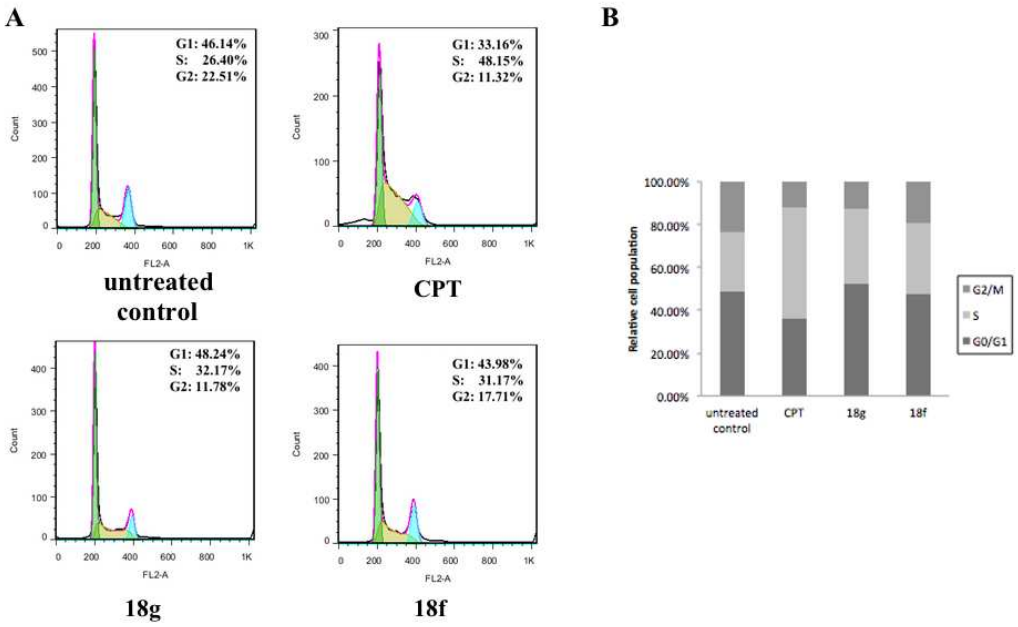

Figure 6. 18f and **18g** induced S phase cell cycle arrest in lung cancer cells. (A) A549 cells were treated with 0.5 μM **18f** and **18g** for 24 h. Cells treated with 0.5 μM **CPT** was used as positive control. (B) Summary of the percentage of cells in S phase.

*2.3.5 Compounds **18f** and **18g** inhibited the growth of A549 tumor xenografts in nude mice*

Tumor xenografts transplanted by A549 cells were used to evaluate the antitumor effect of compounds **18f** and **18g** *in vivo*. The tumor volume in drug-treated mice was less than that in negative control mice at the same measurement day (**Figure 7A**). Values of T/C in the 20 mg/kg **18f** group were 87.18% (day 3), 95.42% (day 6), 85.54% (day 9), 58.03% (day 12), 76.40% (day 15) and 62.96% (day 18), 73.07% (day 21), 74.32% (day 23). And the values of T/C in the 20 mg/kg **18g** group were 140.57% (day 3), 114.41% (day 6), 118.67% (day 9), 85.88% (day 12), 73.12% (day 15) and 68.69% (day 18), 71.52% (day 21), 64.72% (day 23). In Hydroxycamptothecin group, the values of T/C was 91.99% (day 3), 68.37% (day 6), 54.55% (day 9), 29.44% (day 12), 27.97% (day 15) and 23.92% (day 18), 20.00% (day 21), 21.68% (day 23). At the end of the experiment (**Figure 7B** and **7D**), the weight of tumors was reduced by **18f** and **18g,** the inhibitory rate was 29.25% and 42.75%, respectively. Meanwhile, the body weight of the mice in the **18f** and **18g** groups remained essentially unchanged compared with 20 mg/kg Hydroxycamptothecin (**Figure 7C**) and none of the mice died during the treatment, which suggested compounds **18f** and **18g** possess lower toxicities than Hydroxycamptothecin.

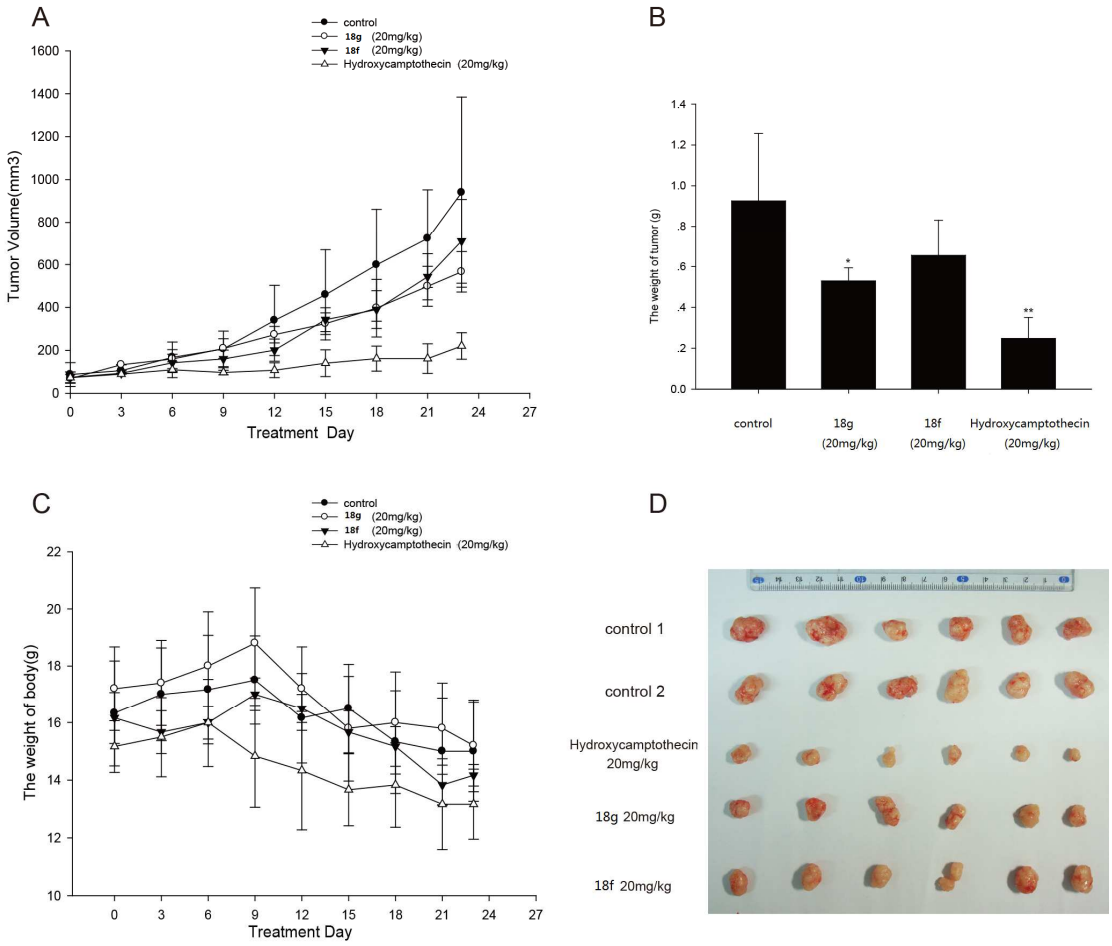

Figure 7. 18f and **18g** inhibited the growth of A549 transplantable tumors. (A) Tumor volume of control, **18f**, **18g** and Hydroxycamptothecin-treated group. (B) The weight of tumor of control, **18f**, **18g** and Hydroxycamptothecin-treated group. *$P < 0.05$, ** $P < 0.01$ compared with control. (C) The body weight of the control group and drug-treated groups. (D) The photograph of tumors.

3. Conclusion

In summary, 17 novel quinolone derivatives were designed and synthesized. Their antitumor activities and Top I inhibitory effects *in vitro* were detected. As a result, two compounds - **18f** and **18g** exhibited potent activities as strong as **CPT**. Furthermore, Compounds **18f** and **18g** led to an obvious increase in percentage of A549 cells in S phase at 24 h treatment. The results *in vivo* showed that **18f** and **18g** had less morbidity and a change in body weight compared with Hydroxycamptothecin. Further research about the biological activities and other molecular mechanism of these potent compounds are currently going on in our group.

4. Experimental procedures

4.1 Chemistry

All reagents were from commercial sources. With tetramethylsilane (TMS) as internal standard,

the ^{1}H NMR and ^{13}C NMR were recorded on Bruker AV-300 apparatus by using deuterated solvents. HR-MS was collected on Agilent technologies 6520 Accurate-Mass Q-TOF LC/MS instruments. Melting points were measured by XT-4 melting point apparatus.

*4.1.1 Typical procedure for the preparation of 1-ethyl-6-fluoro-7-(piperazin-1-yl)quinolin-4(1H)-one (**8**), 1-cyclopropyl-6-fluoro-7-(piperazin-1-yl)quinolin-4(1H)-one (**9**)*

To the stirred solution of 200 ml concentrated hydrochloric acid, norfloxacin (**6**, 20 g, 62.70 mmol) or ciprofloxacin (**7**, 20 g, 60.42 mmol) was added. After stirred and refluxed for 24h, the mixture was cooled down, **8** and **9** were obtained by the vacuum distillation.

*4.1.2 Typical procedure for the preparation of 3-bromo-1-ethyl-6-fluoro-7-(piperazin-1-yl)quinolin-4 (1H)-one (**10**), 3-bromo-1-cyclopropyl-6-fluoro-7-(piperazin-1-yl)quinolin-4(1H)-one (**11**)*

To a solution of compounds **8** (20 g, 44.15 mmol) or **9** (20 g, 43.01 mmol) in 200 ml AcOH, 3.9 ml Br_2 which was diluted by 20 ml AcOH was slowly added. After stirred in 25 □ overnight, the mixture was filtrated and washed with EA (50 ml × 3) to yield compounds **10**, **11**.

*4.1.3 Typical procedure for the preparation of tert-butyl 4-(3-bromo-1-ethyl-6-fluoro-4-oxo-1,4-dihydroquinolin-7-yl)piperazine-1-carboxylate (**12**), tert-butyl 4-(3-bromo-1-cyclopropyl-6-fluoro-4-oxo-1,4-dihydroquinolin-7-yl)piperazine-1-carboxylate (**13**)*

To a solution of compounds **10** (20 g, 72.73 mmol) or **11** (20 g, 69.67 mmol) in 200 ml CH_2Cl_2, 17 ml $(Boc)_2O$ (16 ml for **11**) which was diluted by 20 ml CH_2Cl_2 was slowly added, then 1ml Et_3N was added. After stirred at 25 □ overnight, the mixture was filtrated and washed with CH_2Cl_2 (50 ml × 3) to yield compounds **12**, **13**.

*4.1.4 Typical procedure for the preparation of 3-bromo-1-cyclopropyl-6-fluoro-7-(4-methylpiperazin-1-yl)quinolin-4(1H)-one (**14**)*

Compound **11** (2 g, 6.97 mmol) was dissolved with 20 ml MeOH, ICH_3 (7.67 mmol) and NaOMe (7.67 mmol) were slowly added at -10 □, After stirred overnight under N_2, the solvent was concentrated in vacuo, then 20 ml of water was added, the mixture was extracted with $CHCl_3$ (20 ml × 3). The combined organic layer was dried with anhydrous Na_2SO_4 and the product was obtained after purification with PE:EA=30:1 by column chromatography.

*4.1.5 Typical procedure for the preparation of **15a-g**, **16**a-g, **18h-i***

To a solution of compounds **12-14** (1 g, 2.2 mmol for **12**, **13**, 2.6 mmol for **14**) and phenylboronic acid derivatives (2.4 mmol for **12**, **13**, 2.9 mmol for **14**) in 20 ml toluene, 10 ml methanol and 3 ml water, K_2CO_3 (5.5 mmol for **12**, **13**, 6.5 mmol for **14**) and $Pd(PPh_3)_4$ (0.01 g) were added. After stirred and refluxed 2 h under N_2, the mixture was filtrated and washed with methanol, the solvent was removed by reduced pressure distillation, and methanol was added to dissolve the solid. The mixture was filtrated again washed with methanol to remove the K_2CO_3 and $Pd(PPh_3)_4$, then the solvent was

removed by reduced pressure distillation. Recrystallized in acetonitrile to gave compounds **15a-h**, **16a-g**, **18h-i** in yields of 80-90%.

*4.1.6 Typical procedure for the preparation of **17a-h**, **18a-g***

Compounds **15a-h**, **16a-g (**1 g**)**were dissolved with 10 ml AcOH, after stirred and refluxed for 6 h, the solution was cooled down and adjusted to pH=8 with 25% NaOH. The mixture was filtrated and washed with ice water (10 ml × 3) to give compounds **17a-h**, **18a-g** in yield of 80-90%.

*4.1.6.1 1-ethyl-6-fluoro-3-phenyl-7-(piperazin-1-yl)quinolin-4(1H)-one (**17a**)*

It was obtained as a white solid in 87.1% yield. m.p. 228-229 °C, HRMS (ESI): m/z, calculated for $C_{21}H_{22}FN_3O$, 352.1747 $(M+H)^+$, found 352.1808; ^{1}H NMR (300 MHz, DMSO-d_6): δ 8.27 (s, 1H, 5-H), 7.90 (s, 1H, 2-H), 7.74 (t, 2H, *J* = 7.2 Hz, Ar-H), 7.39 (d, 2H, *J* = 8.0 Hz, Ar-H), 7.30 (t, 1H, *J* = 8.9 Hz, Ar-H), 7.06 (s, 1H, 8-H), 4.40 (q, 2H, *J* = 7.7 Hz, N-CH_2), 3.66 (t, 4H, *J* = 4.9 Hz, 2×CH_2), 3.22 (t, 4H, *J* = 4.5 Hz, 2×CH_2), 1.40 (t, 3H, *J* = 6.7 Hz, N-$CH_2\underline{CH_3}$); ^{13}C NMR (75 MHz, DMSO-d_6): δ 172.3, 159.5, 153.5, 150.0, 144.4, 142.7, 136.6, 132.9, 130.2, 118.8, 114.2, 111.3, 104.6, 51.0, 47.4, 45.5, 14.2 ppm.

*4.1.6.2 1-ethyl-6-fluoro-3-(4-fluorophenyl)-7-(piperazin-1-yl)quinolin-4(1H)-one (**17b**)*

It was obtained as a white solid in 85.6% yield. m.p. 229-230 °C, HRMS (ESI): m/z, calculated for $C_{21}H_{21}F_2N_3O$, 370.1653 $(M+H)^+$, found 370.1707; ^{1}H NMR (300 MHz, DMSO-d_6): δ 8.29 (s, 1H, 5-H), 7.87 (s, 1H, 2-H), 7.80 (d, 2H, *J* = 8.8 Hz, Ar-H), 7.22 (d, 2H, *J* = 8.9 Hz, Ar-H), 7.06 (s, 1H, 8-H), 4.40 (q, 2H, *J* = 6.9 Hz, N-CH_2), 3.66 (t, 4H, *J* = 4.4 Hz, 2×CH_2), 3.22 (t, 4H, *J* = 4.8 Hz, 2×CH_2), 1.40 (t, 3H, *J* = 7.0 Hz, N-$CH_2\underline{CH_3}$); ^{13}C NMR (75 MHz, DMSO-d_6): δ 172.8, 159.3, 153.7, 150.5, 144.6, 142.4, 136.3, 132.0, 130.2, 118.0, 114.7, 111.5, 104.6, 51.0, 47.3, 45.5, 14.2 ppm.

*4.1.6.3 3-(4-chlorophenyl)-1-ethyl-6-fluoro-7-(piperazin-1-yl)quinolin-4(1H)-one (**17c**)*

It was obtained as a white solid in 83.2% yield. m.p. 229-230 °C, HRMS (ESI): m/z, calculated for $C_{21}H_{21}ClFN_3O$, 386.1357 $(M+H)^+$, found 386.1419; ^{1}H NMR (300 MHz, DMSO-d_6): δ 8.33 (s, 1H, 5-H), 7.87 (s, 1H, 2-H), 7.82 (d, 2H, *J* = 8.5 Hz, Ar-H), 7.45 (d, 2H, *J* = 8.4 Hz, Ar-H), 7.06 (s, 1H, 8-H), 4.40 (q, 2H, *J* = 7.6 Hz, N-CH_2), 3.66 (t, 4H, *J* = 4.9 Hz, 2×CH_2), 3.22 (t, 4H, *J* = 4.7 Hz, 2×CH_2), 1.40 (t, 3H, *J* = 6.8 Hz, N-$CH_2\underline{CH_3}$); ^{13}C NMR (75 MHz, DMSO-d_6): δ 172.6, 160.7, 153.7, 150.4, 144.5, 142.6, 136.3, 134.6, 129.9, 127.7, 117.6, 111.5, 104.6, 51.0, 47.4, 45.4, 14.2 ppm.

*4.1.6.4 1-ethyl-6-fluoro-3-(4-methoxyphenyl)-7-(piperazin-1-yl)quinolin-4(1H)-one (**17d**)*

It was obtained as a white solid in 81.8% yield. m.p. 227-228 °C, HRMS (ESI): m/z, calculated for $C_{22}H_{24}ClFN_3O_2$, 382.1853 $(M+H)^+$, found 382.1911; ^{1}H NMR (300 MHz, DMSO-d_6): δ 8.20 (s, 1H, 5-H), 7.85 (s, 1H, 2-H), 7.68 (d, 2H, *J* = 8.8 Hz, Ar-H), 7.04 (s, 1H, 8-H), 6.95 (d, 2H, *J* = 8.8 Hz, Ar-H), 4.39 (q, 2H, *J* = 7.4 Hz, N-CH_2), 3.78 (s, 3H, -OCH_3), 3.65 (t, 4H, *J* = 4.4 Hz, 2×CH_2), 3.20 (t, 4H, *J* = 4.7 Hz, 2×CH_2), 1.38 (t, 3H, *J* = 7.9 Hz, N-$CH_2\underline{CH_3}$); ^{13}C NMR (75 MHz, DMSO-d_6): δ 172.8,

158.0, 153.6, 150.4, 144.5, 141.8, 136.2, 129.4, 128.0, 118.9, 113.2, 111.5, 104.5, 55.0, 51.1, 47.2, 45.5, 14.2 ppm.

*4.1.6.5 4-(1-ethyl-6-fluoro-4-oxo-7-(piperazin-1-yl)-1,4-dihydroquinolin-3-yl)benzonitrile (**17e**)*

It was obtained as a white solid in 86.7% yield. m.p. 228-229 °C, HRMS (ESI): m/z, calculated for $C_{22}H_{21}FN_4O$, 377.1699 $(M+H)^+$, found 377.1756; ^{1}H NMR (300 MHz, DMSO-d_6): δ 8.45 (s, 1H, 5-H), 8.04 (d, 2H, *J* = 8.2 Hz, Ar-H), 7.88 (d, 2H, *J* = 8.1 Hz, Ar-H), 7.83 (s, 1H, 2-H), 7.07 (s, 1H, 8-H), 4.42 (q, 2H, *J* = 7.7 Hz, N-CH_2), 3.65 (t, 4H, *J* = 4.8 Hz, 2×CH_2), 3.25 (t, 4H, *J* = 4.4 Hz, 2×CH_2), 1.40 (t, 3H, *J* = 6.8 Hz, N-$CH_2\underline{CH_3}$); ^{13}C NMR (75 MHz, DMSO-d_6): δ 172.6, 153.8, 150.6, 144.7, 143.6, 140.8, 136.2, 128.5, 121.1, 119.2, 116.7, 111.6, 108.4, 104.7, 50.9, 47.6, 45.4, 14.2 ppm.

*4.1.6.6 1-ethyl-6-fluoro-3-(3-fluorophenyl)-7-(piperazin-1-yl)quinolin-4(1H)-one (**17f**)*

It was obtained as a white solid in 84.3% yield. m.p. 229-230 °C, HRMS (ESI): m/z, calculated for $C_{21}H_{21}F_2N_3O$, 370.1653 $(M+H)^+$, found 370.1707; ^{1}H NMR (300 MHz, DMSO-d_6): δ 8.38 (s, 1H, 5-H), 7.89 (s, 1H, 2-H), 7.71 (t, 1H, *J* = 9.3 Hz, Ar-H), 7.64 (d, 1H, *J* = 10.4 Hz, Ar-H), 7.42 (d, 1H, *J* = 9.3 Hz, Ar-H), 7.12 (s, 1H, Ar-H), 7.07 (s, 1H, 8-H), 4.40 (q, 2H, *J* = 8.0 Hz, N-CH_2), 3.66 (t, 4H, *J* = 4.4 Hz, 2×CH_2), 3.22 (t, 4H, *J* = 4.5 Hz, 2×CH_2), 1.40 (t, 3H, *J* = 6.7 Hz, N-$CH_2\underline{CH_3}$); ^{13}C NMR (75 MHz, DMSO-d_6): δ 172.8, 163.5, 160.2, 153.7, 150.5, 144.9, 143.0, 138.5, 136.3, 129.6, 123.9, 114.8, 113.1, 111.6, 104.6, 51.1, 47.5, 45.5, 14.2 ppm.

*4.1.6.7 3-(3-chlorophenyl)-1-ethyl-6-fluoro-7-(piperazin-1-yl)quinolin-4(1H)-one (**17g**)*

It was obtained as a white solid in 82.5% yield. m.p. 229-230 °C, HRMS (ESI): m/z, calculated for $C_{21}H_{21}ClFN_3O$, 386.1357 $(M+H)^+$, found 386.1419; ^{1}H NMR (300 MHz, DMSO-d_6): δ 8.38 (s, 1H, 5-H), 7.91 (s, 1H, 2-H), 7.87 (s, 1H, Ar-H), 7.76 (t, 1H, *J* = 7.9 Hz, Ar-H), 7.44 (d, 1H, *J* = 7.9 Hz, Ar-H), 7.35 (d, 1H, *J* = 8.8 Hz, Ar-H), 7.07 (s, 1H, 8-H), 4.40 (q, 2H, *J* = 7.3 Hz, N-CH2), 3.66 (t, 4H, *J* = 4.4 Hz, 2×CH_2), 3.22 (t, 4H, *J* = 4.9 Hz, 2×CH_2), 1.40 (t, 3H, *J* = 7.0 Hz, N-$CH_2\underline{CH_3}$); ^{13}C NMR (75 MHz, DMSO-d_6): δ 172.7, 163.5, 160.5, 153.8, 150.7, 144.8, 143.1, 138.5, 136.4, 129.6, 123.8, 114.6, 113.2, 111.5, 104.6, 51.1, 47.5, 45.5, 14.2 ppm.

*4.1.6.8 1-ethyl-6-fluoro-3-(4-methoxyphenyl)-7-(piperazin-1-yl)quinolin-4(1H)-one (**17h**)*

It was obtained as a white solid in 85.2% yield. m.p. 227-228 °C, HRMS (ESI): m/z, calculated for $C_{22}H_{24}FN_3O_2$, 382.1853 $(M+H)^+$, found 382.1911; ^{1}H NMR (300 MHz, DMSO-d_6): δ 8.29 (s, 1H, 5-H), 7.87 (s, 1H, 2-H), 7.38 (t, 1H, *J* = 8.1 Hz, Ar-H), 7.31 (d, 1H, *J* = 6.0 Hz, Ar-H), 7.26 (s, 1H, Ar-H), 7.05 (d, 1H, *J* = 7.0 Hz, Ar-H), 6.86 (s, 1H, 8-H), 4.40 (q, 2H, *J* = 7.8 Hz, N-CH_2), 3.78 (s, 3H, -OCH_3), 3.66 (t, 4H, *J* = 4.9 Hz, 2×CH_2), 3.21 (t, 4H, *J* = 4.5 Hz, 2×CH_2), 1.39 (t, 3H, *J* = 6.9 Hz, N-$CH_2\underline{CH_3}$); ^{13}C NMR (75 MHz, DMSO-d_6): δ 172.9, 158.8, 153.6, 150.4, 144.5, 142.6, 137.1, 136.2, 128.7, 120.5, 118.8, 114.0, 111.6, 111.3, 104.5, 54.9, 51.0, 47.3, 45.5, 14.2 ppm.

*4.1.6.9 1-cyclopropyl-6-fluoro-3-phenyl-7-(piperazin-1-yl)quinolin-4(1H)-one (**18a**)*

It was obtained as a white solid in 89.4% yield. m.p. 268-269 °C, HRMS (ESI): m/z, calculated for $C_{22}H_{22}FN_3O$, 364.1747 $(M+H)^+$, found 364.1828; ^{1}H NMR (300 MHz, DMSO-d_6): δ 8.18 (s, 1H, 5-H), 7.84 (s, 1H, 2-H), 7.79 (t, 1H, *J* = 7.3 Hz, Ar-H), 7.70 (s, 1H, 8-H), 7.42 (t, 2H, *J* = 7.6 Hz, Ar-H), 7.38 (d, 2H, *J* = 7.7 Hz, Ar-H), 3.64 (m, 1H, N-CH), 3.18 (t, 4H, *J* = 4.9 Hz, 2×CH_2), 2.94 (t, 4H, *J* = 4.9 Hz, 2×CH_2), 1.24 (m, 2H, N-CHC$\underline{H_2}$), 1.17 (m, 2H, N-CHC$\underline{H_2}$); ^{13}C NMR (75 MHz, DMSO-d_6): δ 169.0, 145.3, 144.0, 138.4, 132.7, 129.0, 128.5, 128.0, 119.6, 117.9, 110.6, 110.3, 105.9, 46.1, 42.7, 36.0, 7.7 ppm.

*4.1.6.10 1-cyclopropyl-6-fluoro-3-(4-fluorophenyl)-7-(piperazin-1-yl)quinolin-4(1H)-one (**18b**)*

It was obtained as a white solid in 89.9% yield. m.p. 266-267 °C, HRMS (ESI): m/z, calculated for $C_{22}H_{21}F_2N_3O$, 382.1653 $(M+H)^+$, found 382.1722; ^{1}H NMR (300 MHz, DMSO-d_6): δ 8.03 (s, 1H, 5-H), 7.81 (s, 1H, 2-H), 7.74 (d, 2H, *J* = 7.3 Hz, Ar-H), 7.39 (s, 1H, 8-H), 7.20 (d, 2H, *J* = 7.6 Hz, Ar-H), 3.60 (m, 1H, N-CH), 3.15 (t, 4H, *J* = 4.9 Hz, 2×CH_2), 2.91 (t, 4H, *J* = 4.9 Hz, 2×CH_2), 1.21 (m, 2H, N-CH$\underline{CH_2}$), 1.14 (m, 2H, N-CH$\underline{CH_2}$); ^{13}C NMR (75 MHz, DMSO-d_6): δ 162.6, 144.2, 141.6, 138.3, 131.9, 130.4, 126.5, 124.3, 120.1, 118.0, 114.6, 111.2, 105.2, 50.8, 45.3, 34.0, 7.7 ppm.

*4.1.6.11 3-(4-chlorophenyl)-1-cyclopropyl-6-fluoro-7-(piperazin-1-yl)quinolin-4(1H)-one (**18c**)*

It was obtained as a white solid in 89.9% yield. m.p. 268-269 °C, HRMS (ESI): m/z, calculated for $C_{22}H_{21}ClFN_3O$, 398.1357 $(M+H)^+$, found 398.1444; ^{1}H NMR (300 MHz, DMSO-d_6): δ 8.09 (s, 1H, 5-H), 7.78 (s, 1H, 2-H), 7.76 (s, 1H, 8-H), 7.44 (d, 2H, *J* = 3.9 Hz, Ar-H), 7.41 (d, 2H, *J* = 2.6 Hz, Ar-H), 3.62 (m, 1H, N-CH), 3.17 (t, 4H, *J* = 4.9 Hz, 2×CH_2), 2.92 (t, 4H, *J* = 4.8 Hz, 2×CH_2), 1.23 (m, 2H, N-CH$\underline{CH_2}$), 1.17 (m, 2H, N-CH$\underline{CH_2}$); ^{13}C NMR (75 MHz, DMSO-d_6): δ 152.6, 144.2, 141.8, 138.3, 134.5, 131.0, 130.1, 127.7, 123.2, 117.6, 111.3, 111.0, 105.3, 50.8, 45.3, 34.1, 7.7 ppm.

*4.1.6.12 1-cyclopropyl-6-fluoro-3-(4-methoxyphenyl)-7-(piperazin-1-yl)quinolin-4(1H)-one (**18d**)*

It was obtained as a white solid in 87.2% yield. m.p. 265-266 °C, HRMS (ESI): m/z, calculated for $C_{23}H_{24}FN_3O_2$, 394.1853 $(M+H)^+$, found 394.1923; ^{1}H NMR (300 MHz, DMSO--d_6): δ 7.97 (s, 1H, 5-H), 7.80 (s, 1H, 2-H), 7.64 (d, 2H, *J* = 9.9 Hz, Ar-H), 7.40 (s, 1H, 8-H), 6.95 (d, 2H, *J* = 9.3 Hz, Ar-H), 3.78 (s, 3H, -OCH_3), 3.60 (m, 1H, N-CH), 3.14 (t, 4H, *J* = 4.6 Hz, 2×CH_2), 2.90 (t, 4H, *J* = 4.6 Hz, 2×CH_2), 1.22 (m, 2H, N-CH$\underline{CH_2}$), 1.13 (m, 2H, N-CH$\underline{CH_2}$); ^{13}C NMR (75 MHz, DMSO-d_6): δ 158.0, 155.2, 150.6, 144.1, 140.9, 138.3, 129.6, 127.9, 120.3, 113.3, 111.2, 110.9, 105.2, 55.0, 51.0, 45.5, 33.9, 7.7 ppm.

*4.1.6.13 1-cyclopropyl-6-fluoro-3-(3-fluorophenyl)-7-(piperazin-1-yl)quinolin-4(1H)-one (**18e**)*

It was obtained as a white solid in 84.7% yield. m.p. 266-267 °C, HRMS (ESI): m/z, calculated for $C_{22}H_{21}F_2N_3O$, 382.1653 $(M+H)^+$, found 382.1722; ^{1}H NMR (300 MHz, DMSO-d_6): δ 8.09 (s, 1H, 5-H), 7.78 (s, 1H, 2-H), 7.61 (t, 1H, *J* = 10.1 Hz, Ar-H), 7.50 (s, 1H, 8-H), 7.40 (d, 1H, *J* = 7.4 Hz, Ar-H), 7.38 (s, 1H, Ar-H), 7.17 (d, 1H, *J* = 8.2 Hz, Ar-H), 3.60 (m, 1H, N-CH), 3.19 (t, 4H, *J* = 4.6 Hz,

2×CH_2), 2.94 (t, 4H, *J* = 4.4 Hz, 2×CH_2), 1.23 (m, 2H, N-CH$\underline{CH_2}$), 1.15 (m, 2H, N-CH$\underline{CH_2}$); ^{13}C NMR (75 MHz, DMSO-d_6): δ 162.4, 144.3, 142.1, 138.5, 130.0, 129.6, 129.5, 124.2, 124.1, 120.0, 119.8, 116.9, 115.1, 114.8, 105.4, 50.8, 45.4, 34.2, 7.7 ppm.

4.1.6.14 3-(3-chlorophenyl)-1-cyclopropyl-6-fluoro-7-(piperazin-1-yl)quinolin-4(1H)-one ***(18f)***

It was obtained as a white solid in 86.8% yield. m.p. 268-269 °C, HRMS (ESI): m/z, calculated for $C_{22}H_{21}ClFN_3O$, 398.1357 $(M+H)^+$, found 398.1444; ^{1}H NMR (300 MHz, DMSO-d_6): δ 8.13 (s, 1H, 5-H), 7.86 (s, 1H, 2-H), 7.79 (d, 1H, *J* = 8.5 Hz, Ar-H), 7.68 (t, 1H, *J* = 7.9 Hz, Ar-H), 7.43 (s, 1H, 8-H), 7.41 (s, 1H, Ar-H), 7.33 (d, 1H, *J* = 7.1 Hz, Ar-H), 3.63 (m, 1H, N-CH), 3.17 (t, 4H, *J* = 4.4 Hz, 2×CH_2), 2.91 (t, 4H, *J* = 4.0 Hz, 2×CH_2), 1.23 (m, 2H, N-CH$\underline{CH_2}$), 1.17 (m, 2H, N-CH$\underline{CH_2}$); ^{13}C NMR (75 MHz, DMSO-d_6): δ 162.2, 144.1, 142.2, 138.3, 137.8, 133.5, 132.5, 129.6, 129.5, 128.0, 126.8, 126.2, 118.4, 111.3, 105.3, 50.8, 45.4, 34.2, 7.7 ppm.

4.1.6.15 1-cyclopropyl-6-fluoro-3-(3-methoxyphenyl)-7-(piperazin-1-yl)quinolin-4(1H)-one ***(18g)***

It was obtained as a white solid in 88.8% yield. m.p. 265-266 °C, HRMS (ESI): m/z, calculated for $C_{23}H_{24}FN_3O_2$, 394.1853 $(M+H)^+$, found 394.1923; ^{1}H NMR (300 MHz, DMSO-d_6): δ 8.06 (s, 1H, 5-H), 7.77 (s, 1H, 2-H), 7.40 (t, 1H, *J* = 7.5 Hz, Ar-H), 7.31 (s, 1H, 8-H), 7.26 (s, 1H, Ar-H), 7.23 (d, 1H, *J* = 6.3 Hz, Ar-H), 6.85 (d, 1H, *J* = 6.0 Hz, Ar-H), 3.78 (s, 3H, -OCH_3), 3.60 (m, 1H, N-CH), 3.16 (t, 4H, *J* = 4.5 Hz, 2×CH_2), 2.92 (t, 4H, *J* = 4.2 Hz, 2×CH_2), 1.23 (m, 2H, N-CH$\underline{CH_2}$), 1.15 (m, 2H, N-CH$\underline{CH_2}$); ^{13}C NMR (75 MHz, DMSO-d_6): δ 173.0, 158.9, 153.6, 150.8, 144.2, 141.7, 138.2, 128.7, 120.7, 118.8, 114.2, 112.0, 111.3, 111.0, 105.2, 55.0, 50.8, 45.3, 34.0, 7.7 ppm.

4.1.6.16 3-(3-chlorophenyl)-1-cyclopropyl-6-fluoro-7-(4-methylpiperazin-1-yl)quinolin-4(1H)-one ***(18h)***

It was obtained as a white solid in 88.4% yield. m.p. 268-269 °C, HRMS (ESI): m/z, calculated for $C_{23}H_{23}ClFN_3O$, 412.1514 $(M+H)^+$, found 412.1604; ^{1}H NMR (300 MHz, DMSO-d_6): δ 8.15 (s, 1H, 5-H), 7.90 (s, 1H, 2-H), 7.76 (d, 1H, *J* = 8.5 Hz, Ar-H), 7.65 (t, 1H, *J* = 7.9 Hz, Ar-H), 7.48 (s, 1H, 8-H), 7.42 (s, 1H, Ar-H), 7.30 (d, 1H, *J* = 7.1 Hz, Ar-H), 3.63 (m, 1H, N-CH), 3.17 (t, 4H, *J* = 4.4 Hz, 2×CH_2), 2.91 (t, 4H, *J* = 4.0 Hz, 2×CH_2), 2.23 (s, 3H, N-CH_3), 1.23 (m, 2H, N-CH$\underline{CH_2}$), 1.17 (m, 2H, N-CH$\underline{CH_2}$); ^{13}C NMR (75 MHz, DMSO-d_6): δ 162.2, 144.1, 142.2, 138.3, 137.8, 133.5, 132.5, 129.6, 129.5, 128.0, 126.8, 126.2, 118.4, 111.3, 105.3, 50.8, 45.4, 40.6, 34.2, 7.7 ppm.

4.1.6.17 1-cyclopropyl-6-fluoro-3-(3-methoxyphenyl)-7-(4-methylpiperazin-1-yl)quinolin-4(1H)-one ***(18i)***

It was obtained as a white solid in 87.1% yield. m.p. 265-266 °C, HRMS (ESI): m/z, calculated for $C_{24}H_{26}FN_3O_2$, 407.2009 $(M+H)^+$, found 407.2073; ^{1}H NMR (300 MHz, DMSO-d_6): δ 8.16 (s, 1H, 5-H), 7.75 (s, 1H, 2-H), 7.43 (t, 1H, *J* = 7.5 Hz, Ar-H), 7.30 (s, 1H, 8-H), 7.25 (s, 1H, Ar-H), 7.20 (d, 1H, *J* = 6.3 Hz, Ar-H), 6.85 (d, 1H, *J* = 6.0 Hz, Ar-H), 3.78 (s, 3H, -OCH_3), 3.60 (m, 1H, N-CH), 3.16

(t, 4H, *J* = 4.5 Hz, 2×CH_2), 2.92 (t, 4H, *J* = 4.2 Hz, 2×CH_2), 2.23 (s, 3H, N-CH_3), 1.23 (m, 2H, N-CH$\underline{CH_2}$), 1.15 (m, 2H, N-CH$\underline{CH_2}$); ^{13}C NMR (75 MHz, DMSO-d_6): δ 173.0, 158.9, 153.6, 150.8, 144.2, 141.7, 138.2, 128.7, 120.7, 118.8, 114.2, 112.0, 111.3, 111.0, 105.2, 55.0, 50.8, 45.3, 40.6, 34.0, 7.7 ppm.

4.2 Docking study

Glide was selected as the molecular docking tool. The crystallized complex structure of Top I (PDB ID: 1K4T) was prepared using the Protein PreparationWizard workflow. A receptor grid was generated on the center of the co-crystallized ligand, which was defined as the ligand-binding site search region. The compound to be docked was confirmed by an enclosing box that was similar in size to the co-crystallized ligand. Furthermore, the compound set was minimized using the LigPrep module. The best conformation of each compound was output on the basis of the Glide score and interactions formed between the compounds and the active site. Finally, the potential compounds were flexibly docked into the binding site using the extra precision (XP) docking mode. All the remaining parameters were kept as default.

4.3 Biology

4.3.1 Cytotoxicity of quinolone derivatives in various human cancer cell lines.

Cells were seeded into a 96-well plate at 6×10^4 to 8×10^4 cells per well and incubated for 24h. Over a range of concentrations from 0.01 to 100 μM, all compounds were added and treated for 48 h. 20 μl of MTT solution were added to each well, and plates were incubated for 4 h. DMSO (150 μl) was added to each well and shaken ten minutes in shaking table to dissolve the Formazan crystals. The absorbance (at wavelength of 570 nm) was measured on an enzyme-linked immunosorbent detector. Then the cytotoxicity IC_{50} values, which are the concentrations leading to 50% cell death *in vitro*, were obtained.

4.3.2 Top I inhibition assay.

Reaction mixtures 20 μl final volume contained 1 μl (0.25 μg/ul) of supercoile pBR322 DNA in the 10×Tris/Glycine/SDS (TGS) buffer (10 mM Tris-HCl, pH 7.9, 0.15M NaCl, 10% BSA, 1 mM EDTA, 0.1 mM Spermidine, 5% glycerol.), 3-5 units Top 1, 5 μl compounds and appropriate distilled water to make the final reaction volumes 20 μl. Reactions were incubated at 37 °C for 30 min and terminated by the addition of 2 μl 10% SDS (0.1 volume), and then proteinase K was added to 50 μg/ml. The reactions were digested at 37 °C for 30 min. 2 μl of loading buffer (0.25% Bromophenol Blue, 50% glycerol, 0.1 volume) was then added. Aliquots of 20 μl were subjected to electrophoresis in 1% agarose gel at 60 V for 2.5 h in 1×Tris/acetate (TAE) buffer (20 mM Tris-acetate, 0.5 mM EDTA, pH 8.3). After electrophoresis, DNA bands were stained in 0.5 mg/mL of ethidium bromide and visualized by transillumination with UV light (510 nm).

4.3.3 Flow cytometry for DNA content analysis.

A549 cells were seeded into a 6-well plate at 2.5×10^5 cells per well. The cells were incubated for 24 h in medium with 0.5% FBS and synchronized with serum-free medium for 12 h, then treated with 0.5 μM **CPT** or **18f** or **18g** for another 24 h. Then the cells were harvested and fixed in cold 70% ethanol over night at 4□. After washing with PBS, the cells were incubated with 100 ml RNaseA (KeyGEN, Nanjing, China) at 37□ for 30 min. Subsequently, the cells were incubated with 400 ml PI (KeyGEN, Nanjing, China) for 30 min at 4□ in the dark and analyzed by flow cytometry (Becton Dickinson, California).

4.3.4 In vivo activity of **18f** and **18g** against human tumor xenografts in nude mice

This study was approved by the SPF Animal Laboratory of China Pharmaceutical University. Five-to six-week-old male BALB/c nude mice were purchased from SLAC Laboratory Animals (Shanghai, China) and were raised in air-conditioned rooms under controlled lighting(12h light/day) and were fed with standard laboratory food and water ad libitum. A549 tumors were induced in the mice by subcutaneously injecting of A549 cells (5.0×10^6) into the flanks of the mice. After 12-14 days, tumor sizes were determined using micrometer calipers, and then the mice with similar tumor volumes (eliminating mice with tumors that were too large or too small) were randomly divided into five groups (with six nude mice per group). The mice were treated with **18f** (20 mg/kg), **18g** (20 mg/kg) and Hydroxycamptothecin (20 mg/kg). The negative group received 0.9% normal saline. Treatments were done by intravenous injection at a frequency of once every 3 days. At the end of 23 days, the mice were sacrificed, and the tumor xenografts were removed and measured .Tumor volume (TV) was calculated every 3 days using the following formula: $TV(mm^3)=D/2\times d^2$, where d and D are the shortest and the longest diameters, respectively. At the same time the animals were weighed twice per week and monitored for mortality throughout the experimental period to assess toxicity of the treatments. Relative tumor volume (RTV) was calculated according to the equation $RTV=V_t/V_0$, where V_0 is the tumor volume at day 0 and V_t is the tumor volume at day t. And the evaluation index for inhibition was the relative tumor growth ratio $T/C=T_{RTV}/C_{RTV}\times100\%$, where T_{RTV} and C_{RTV} represent the RTV of the treated and control groups, respectively.

Acknowledgements

This work was supported by Research Grants 21372260 to Z.-Y.L. from the National Natural Science Foundation (NSFC) of China.

References

1. Redinbo, M. R.; Stewart, L.; Kuhn, P.; Champoux, J. J.; Hol, W. G. Crystal Structures of Human Topoisomerase I in Covalent and Noncovalent Complexes with DNA. *Science*. **1998**, *279*, 1504-1513.

2. Nguyen, T. X.; Morrell, A.; Conda-Sheridan, M.; Marchand, C.; Agama, K.; Bermingam, A.; Stephen, A. G.; Chergui, A.; Naumova, A.; Fisher, R.; O'Keefe, B. R.; Pommier, Y.; Cushman, M. Synthesis and Biological Evaluation of the First Dual Tyrosyl-DNA Phosphodiesterase I (Tdp1)−Topoisomerase I (Top1) Inhibitors. *J. Med. Chem*. **2012**, *55*, 4457−4478.

3. You, Q. D.; Li, Z. Y.; Huang, C. H.; Yang, Q.; Wang, X. J.; Guo, Q. L.; Chen, X. G.; He, X. G.; Li, K. T.; Chern, J. W. Discovery of a Novel Series of Quinolone and Naphthyridine Derivatives as Potential Topoisomerase I Inhibitors by Scaffold Modif ication. *J. Med. Chem.* **2009**, *52*, 5649-5661.

4. Takimoto, C.H.; Wright, J.; Arbuck, S.G. Clinical applications of the camptothecins. *Biochim. Biophys. Acta*. **1998**, *1400*, 107–119.

5. Garcia-Carbonero, R.; Supko, J. G. Clin. Current perspectives on the clinical experience, pharmacology, and continued development of the camptothecins. *Cancer Res*. **2002**, *8*, 641-661.

6. Morrell, A.; Antony, S.; Kohlhagen, G.; Pommier, Y.; Cushman, M. Synthesis of nitrated indenoisoquinolines as topoisomerase I inhibitors. *Bioorg. Med. Chem. Lett.* **2004**, *14*, 3659-3663.

7. Nagarajan, M.; Morrell, A.; Ioanoviciu, A.; Antony, S.; Kohlhagen, G.; Agama, K.; Hollingshead, M.; Pommier, Y.; Cushman, M. Synthesis and Evaluation of Indenoisoquinoline Topoisomerase I Inhibitors Substituted with Nitrogen Heterocycles. *J. Med. Chem.* **2006**, *49*, 6283-6289.

8. Zhang, J. P.; Huang, J.; Liu, C.; Lu, X. F.; Wu, B. X.; Zhao, L.; Lu, N.; Guo, Q. L.; Li, Z. Y.; Jiang, C. Discovery of a series of pyridopyrimidine derivatives as potential topoisomerase I inhibitors. *Chin. Chem. Lett.* **2014**, *25*, 1025-1028.

9. Fox, B. M.; Xiao, X.; Antony, S.; Kohlhagen, G.; Pommier, Y.; Staker, B. L.; Stewart, L.; Cushman, M. Design, synthesis, and biological evaluation of cytotoxic 11-alkenylindenoisoquinoline topoisomerase I inhibitors and indenoisoquinoline-camptothecin hybrids. *J. Med. Chem.* **2003**, *46*, 3275-3282.

10. Morrell, A.; Antony, S.; Kohlhagen, G.; Pommier, Y.; Cushman, M. A systematic study of nitrated indenoisoquinolines reveals a potent topoisomerase I inhibitor. *J. Med. Chem.* **2006**, *49*, 7740-7753.

11. Pommier, Y.; Topoisomerase I inhibitors: camptothecins and beyond. *Nat. Rev. Cancer.* **2006**, *6*, 789-802.

12. Xiao, X. S.; Antony, S.; Pommier, Y.; Cushman, M.; Total synthesis and biological evaluation of 22-hydroxyacuminatine. *J. Med. Chem.* **2006**, *49*, 1408-1412.

13. Li, Z. Y.; Zhai, F. M.; Zhao, L; Guo, Q. L.; You, Q. D. Design and synthesis of N-methylmaleimide indolocarbazole bearing modified 2-acetamino acid moieties as Topoisomerase I inhibitors. *Bioorg.*

Med. Chem. Lett. **2009**, *19*, 406-409.

14. Zhang, X. Y.; Wang, R.; Zhao, L.; Lu, N.; Wang, J. B.; You, Q. D.; Li, Z. Y.; Guo, Q. L. Synthesis and biological evaluations of novel indenoisoquinolines as topoisomerase I inhibitors. *Bioorg. Med. Chem. Lett.* **2012**, *22*, 1276-1281.

15. Pommier, Y. DNA topoisomerase I inhibitors: chemistry, biology, and interfacial inhibition. *Chem. Rev.* **2009**, *109*, 2894-2902.

16. Ioanoviciu, A.; Antony, S.; Pommier, Y.; Staker, B. L.; Stewart, L.; Cushman, M. Synthesis and Mechanism of Action Studies of a Series of Norindenoisoquinoline Topoisomerase I Poisons Reveal an Inhibitor with a Flipped Orientation in the Ternary DNA-Enzyme-Inhibitor Complex As Determined by X-ray Crystallographic Analysis. *J. Med. Chem*. **2005**, *48*, 4803-4814.

17. Staker, B. L.; Feese, M. D.; Cushman, M.; Pommier, Y.; Zembower, D.; Stewart, L.; Burgin, A. B. Structures of Three Classes of Anticancer Agents Bound to the Human Topoisomerase I-DNA Covalent Complex. *J. Med. Chem.* **2005**, 48, 2336-2345.

18. Marchand, C.; Antony, S.; Kohn, K. W.; Cushman, M.; Ioanoviciu, A.; Staker, B. L.; Burgin, A. B.; Stewart, L.; Pommier, Y. A Novel Norindenoisoquinoline Structure Reveals a Common Interfacial Inhibitor Paradigm for Ternary Trapping of the Topoisomerase I-DNA Covalent Complex. *Mol. Cancer Ther.* **2006**, *5*, 287-295.

19. Holm, C.; Covey, J. M.; Kerrigan, D.; Pommier, Y. Differential requirement of DNA replication for the cytotoxicity of DNA topoisomerase I and II inhibitors in Chinese hamster DC3F cells. *Cancer Res.* **1989**, *49*, 6365–6368.

Figure caption:

Figure 1. Structure of Camptothecin, 10-Hydroxycamptothecin, Irinotecan and Toptecan.

Figure 2. Structure of Rebeccamycin and NSC 314622.

Figure 3. Compound generation by scaffold modification.

Figure 4. Effects of quinolone derivatives on Top I-mediated DNA relaxation activity. (A) Lane 1: marker; Lane 2: Top I + supercoiled pBR322 DNA (ScDNA); Lane 3: Top I + ScDNA + **CPT**; Lane 4: Top I + ScDNA + compound **18a**; Lane 5: Top I + ScDNA + compound **18b**, Lane 6: Top I + ScDNA + compound **18c**; Lane 7: Top I + ScDNA + compound **18d**; Lane 8: Top I + ScDNA + compound **18e**; Lane 9: Top I + ScDNA + compound **18f**; Lane 10: Top I + ScDNA + compound **18g**. (B) Effects of test compounds on Top I-mediated DNA relaxation. The proportion of relaxed DNA to the total DNA was measured by scanning with an imaging system. Bars show the percentage of supercoiled vs relaxed DNA. Marker: product of Tanon, China. r for relax pBR322 DNA and s for supercoiled pBR322 DNA.

Figure 5. Docking results of **CPT** and **18g** with Top I/DNA binary complex. Energy-minimized hypothetical top-ranked binding pose of **CPT** and **18g** (colored by atom type). The stereoview is

programmed for wall-eyed (relaxed) viewing. Top I amino acid residues not involved in bonding interactions have been removed to improve clarity. Hydrogen bonds are indicated by green dashed lines. Pi interactions are indicated by orange lines. Protein and compounds represented in stick model.

Figure 6. 18f and **18g** induced S phase cell cycle arrest in lung cancer cells. (A) A549 cells were treated with 0.5 μM **18f** and **18g** for 24 h. Cells treated with 0.5 μM **CPT** was used as positive control. (B) Summary of the percentage of cells in S phase.

Figure 7. 18f and **18g** inhibited the growth of A549 transplantable tumors. (A) Tumor volume of control, **18f**, **18g** and Hydroxycamptothecin-treated group. (B) The weight of tumor of control, **18f**, **18g** and Hydroxycamptothecin-treated group. *$P < 0.05$, ** $P < 0.01$ compared with control. (C) The body weight of the control group and drug-treated groups. (D) The photograph of tumors.

Scheme caption:

Scheme 1. Synthesis of quinolone derivatives. Reagents and conditions: (a) con.HCl, reflux, 24h, 98%; (b) CH_3COOH, Br_2, 25 □, overnight, 95%; (c) $(Boc)_2O$, Et_3N, CH_2Cl_2, 25 □, overnight, 95%; (d) Toluene, MeOH, H_2O, K_2CO_3, $Pd(PPh_3)_4$, N_2, reflux, 2h, 80-90%; (e) CH_3COOH, reflux, 6h, 80-90%; (f) CH_3I, NaOMe, -10 □, overnight, 60%; (g) Toluene, MeOH, H_2O, K_2CO_3, $Pd(PPh_3)_4$, N_2, reflux, 2h, 80-90%.

Table caption:

Table 1. The structures and the *in vitro* cytotoxic activities of quinolone derivatives.

ACCEPTED MANUSCRIPT

ACCEPTED MANUSCRIPT

Highlights:

- Some of our compounds demonstrate potent Top I inhibitory activity as Camptothecin.
- **18f** and **18g** show comparable ability as Camptothecin in Top I inhibitory activity and celluar inhibitory activity.
- **18f** and **18g** impair the cell cycle progression in the s phase.
- **18f** and **18g** represent more safety compared with hydroxycamptothecin.

ACCEPTED MANUSCRIPT